Experimental investigation of waste cooking oil combustion in a novel turbulent swirl burner

Gy. Hidegh[1], D. Csemány[1], A. Kun-Balog[1], V. Józsa[*, 1], C.T. Chong[2]

[1]Budapest University of Technology and Economics, Faculty of Mechanical Engineering, Department of Energy Engineering, 1111 Budapest, Műegyetem rkp. 3., Hungary
[2]China-UK Low Carbon College, Shanghai Jiao Tong University, Lingang, Shanghai 201306, China

Abstract
The present work focuses on the combustion analysis of waste cooking oil (WCO) biodiesel, a second-generation biofuel. The experiments were performed in a novel turbulent swirl burner, featuring a central plain-jet airblast atomizer. Depending on the combustion air preheating temperature and atomizing pressure, straight and V-shaped flames were achieved. Moreover, certain conditions allowed distributed combustion, a new way to reduce emissions. The novel concept is called Mixture Temperature-Controlled (MTC) combustion. It features a low swirl with central cold air injection to delay ignition, facilitating the formation of a more homogeneous fuel vapor-air mixture. Currently, the equivalence ratio was fixed at 0.8 (4.2% O_2), while both the CO and NO emissions remained below 10 ppm in the maintained distributed combustion mode.

Introduction

The pandemic has seriously affected transportation, fostering reduced fossil fuel consumption while making room for renewables [1]. The most spectacular drop is expected in passenger road vehicles, while freight vehicles are expected to slightly follow this trend in a decade [2]. Decarbonization of transport is a highlighted goal in the European Union to mitigate its severe dependence on imported crude oil [3]. Even though hydrogen research receives outstanding funding, it takes time while commercial products and the corresponding infrastructure will be ready for everyday use. Until that, hydrocarbon fuels have to be used. Consequently, liquid renewable hydrocarbons will play a significant role in the transitory period.

Edible oils are the source of first-generation biofuels. Their production endangers food safety [4], hence, alternative solutions have to be included in the liquid fuel portfolio. A potential source is Waste Cooking Oil (WCO), which is a second-generation biofuel, requiring no arable land to produce. WCO is the cheapest option [5] to produce liquid biofuels. Also, the energy requirement for converting the filtered oil into biodiesel can be as low as 1% by using the ultrasonic technique [6]. Currently, biodiesel is blended to petrol diesel fuel, according to regulations. For instance, the EN590:2017 standard allows 7% FAME-based biodiesel. Even though WCO is available at households and restaurants in a considerable quantity, to efficiently collect it, social campaign and governmental support are required [7]. Nevertheless, domestic reuse of neat WCO as stove fuel is accompanied by notable emissions [8], however, it notably depends on the stove design [9]. Since biodiesels are oxygenated fuels, they show a lower tendency for soot formation than pure hydrocarbons [10]. As for CO and NO_X emissions, WCO-biodiesel in a proper concentration can reduce the concentration of both pollutants [11].

There is ongoing research for ultra-low emission burners. Practically 100% combustion efficiency, low unburnt fuel and CO emissions were all solved in the past century [12]. The only critical pollutant is NO_X in combustion that nearly doubles with each 50 K increase in flame temperature [13]. For this reason, various combustion concepts are under development. The most notable candidate of the past decades is MILD combustion [14], which achieves low NO_X emission by using flue gas recirculation, hence, diluting the combustion air. The heat release rate and the peak temperature are reduced, ultimately leading to marginal emissions yet complete combustion. Nevertheless, employing MILD combustion in aero engines is rather challenging [15]. To provide distributed combustion without exhaust gas recirculation, Mixture Temperature-Controlled (MTC) combustion can be used [16]. In the presently investigated configuration, the cool atomizing medium delays ignition, hence, leaves enough time for complete evaporation and homogeneous mixture formation. The resulting flame features very low luminosity and single-digit CO and NO_X emissions.

After successfully testing diesel-coconut biodiesel blends earlier [17], the less volatile WCO is evaluated since it is a more environmentally friendly fuel. The corresponding investigation allows a better understanding of distributed combustion and the operation of the MTC burner. The primary investigated characteristics are the flame shape, chemiluminescent emission, and pollutant emission. Since atomization is a key part of the MTC burner, the required fuel properties were measured and the atomization characteristics were estimated.

Materials and methods

The density of the samples was measured with pycnometers according to ISO 3507:1999 and ISO 4787:2010 standards. The calibration resulted in 0.1%

* Corresponding author: jozsa.viktor@gpk.bme.hu

uncertainty in the measured volume. The mass of the empty and filled pycnometers was measured with a Sartorius laboratory balance with 0.001 g accuracy, resulting in an average uncertainty of 0.8 kg/m^3. A constant temperature bath was used for temperature control with 2 °C uncertainty. Cannon-Fenske viscometers were placed into the same bath to measure kinematic viscosity according to ASTM D445-06 and ASTM D446-07 standards with an average uncertainty of 0.008 mm^2/s. Pendant droplet method was applied for surface tension measurement with a Krüss DSA30 droplet shape analyzer system, mounted with a Stingray F046B IRF digital camera for recording images of the suspended droplets of the investigated samples. A thermostat provided temperature control of the measurement chamber. However, a slight cooldown of the samples due to heat loss resulted in an uncertainty of 2 °C. Figure 1 shows the investigated fuel samples. Blends of diesel fuel (D) and WCO biodiesel were tested in 25 V/V% steps, noted by BXX, where XX refers to the WCO biodiesel concentration.

Fig. 1. Investigated fuel samples.

Figure 2 shows a sketch of the test system, which is detailed in ref. [17]. The key parameters are summarized in Table 1. The equivalence ratio was a constant value of 0.8, using the O_2 concentration data of the flue gas analyzer. The combustion air preheating temperature, t_{ca}, was varied in the range of 150 to 350 °C, using a PID-controlled air heater unit. The lower boundary was set by the volatility of the diesel fuel (according to the EN590:2017 standard). Above 350 °C, distributed combustion was not observed.

Atomizing gauge pressure, p_g, was the second varied parameter in the range of 0.3 to 0.9 bar. The lower boundary was set by the minimum required pressure to have fine enough spray that is able to evaporate before reaching the flame front. Above 0.9 bar, there was no notable variation observed in the presented flame characteristics, while the lower value ensured a fine spray to avoid droplet combustion. The liquid fuel was supplied from a pressurized tank.

Table 1. Characteristic parameters of the measurements.

Property	Value
Thermal power [kW]	13.3
Air flow rate [kg/h]	20
Equivalence ratio [1]	0.8
Atomizing pressure [bar]	0.3–0.9
Air temperature [°C]	150–350

The flue gas analyzer measured CO and NO concentrations with 3 and 2 ppm uncertainty. The uncertainty of O_2 measurement was 0.1 V/V%. Flame chemiluminescence was measured by a custom spectrometer, having 260–580 nm spectral range and 0.3125 nm resolution.

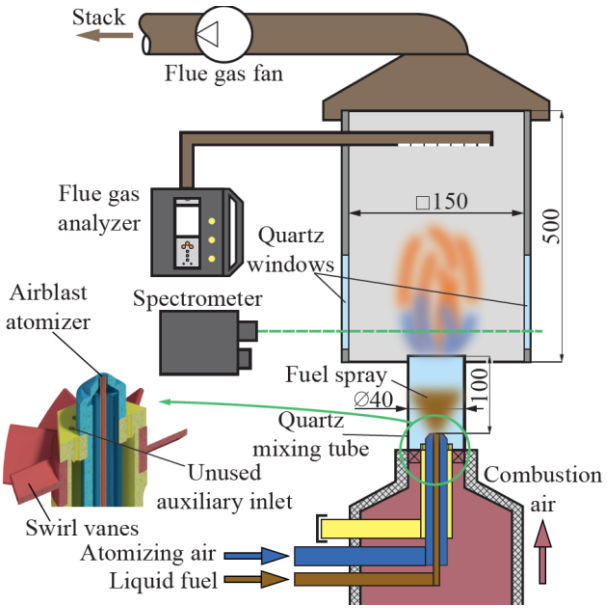

Fig. 2. Sketch of the measurement test rig.

The most relevant value characterizing atomization is the Sauter Mean Diameter, *SMD*. Based on our earlier investigations [18] on airblast atomization, the following expression was used for its estimation:

$$\frac{SMD}{d_0} = (C_1 \cdot \mathrm{We}_A^{-0.5} + C_2 \cdot \mathrm{Oh}) \cdot \left(1 + \frac{1}{AFR}\right), \quad (1)$$

where $d_0 = 0.9$ mm is the fuel jet diameter, *AFR* is the air-to-fuel mass flow ratio, and C_1 and C_2 are empirical constants. We_A is the Weber number, calculated by using the properties of air, and Oh is the Ohnesorge number, calculated as:

$$\mathrm{We}_A = \rho_A \cdot d_0 \cdot w_A^2/\sigma, \quad (2)$$

$$\mathrm{Oh} = \mu_F/(\sigma \cdot d_0 \cdot \rho_F)^{0.5}, \quad (3)$$

where ρ_A is the air density, w_A is the air discharge velocity at the nozzle, and σ is the surface tension. μ_F is the dynamic viscosity of the fuel, and ρ_F is the fuel density.

Results and discussion

The required fuel properties for estimating atomization characteristics are included in Table 2. It contains the measured liquid density (ρ_F), kinematic viscosity (ν_F), and surface tension (σ) of the pure fuels and their blends. The elevated biodiesel content increases all the density, viscosity, and surface tension. Note that σ for B25 is interestingly higher than that of B50. However, B25 showed slight precipitation and greenish color after blending. This behavior and its effects on fuel properties

need further investigations; maybe the fuel preparation was insufficient at the production site. Nevertheless, such precipitation was not observed in any other concentration and other fuel samples from the same manufacturer.

Table 2. Measured fuel properties at 30 °C.

Fuel	ρ_F [kg/m^3]	ν_F [mm^2/s]	σ [mN/m]
D	814.0	2.597	26.24
B25	827.0	3.174	27.17
B50	842.3	3.661	26.9
B75	857.0	4.442	28.35
WCO	871.2	5.570	30.21

The estimated *SMD* of the spray is shown in Fig. 3. Atomizing pressure was the most influential parameter through the Weber number since the air discharge velocity notably increases in the investigated regime. Its values were varied in the range of 712 to 2184, while Oh was varied in the 0.015–0.032 range. The results show that *SMD* increases slightly with the increasing share of biodiesel at all conditions. Since evaporation time scales with the square of the droplet diameter, the investigated range covers a 1:4 evaporation time ratio. A shorter evaporation time is more favorable from the mixing point of view, ultimately leading to reduced pollutant emission.

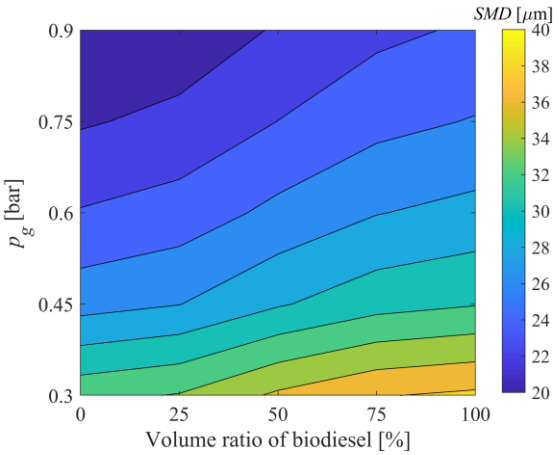

Fig. 3. Estimated *SMD* of blends at 30 °C.

Different flame shapes were observed during the measurements. Figure 4 shows them at each setup. Due to the relatively low volatility of WCO and B75, the fuel droplets could not evaporate properly, making combustion impossible below 200 °C, which is shown as a hatched region. At lower atomizing pressures and combustion air temperatures, straight yellowish flames or V-shaped flames were present. Fifteen typical flame images were selected to show the visual characteristics of typical flames, shown in Fig. 5. The image at the bottom left shows a V-shaped flame of WCO combustion at p_g = 0.3 bar, t_{ca} = 350 °C. However, the weak swirl was not enough to develop a stable V-shaped flame. Interestingly, no V-shaped flames were observed during the combustion of B75. Eventually, for WCO and B75, except p_g = 0.3 bar and t_{ca} = 150 °C, only transitory flames could be observed, meaning an alteration between straight and V flames, marked with pink in Fig. 4. The flame altering between straight and distributed combustion was marked with green color. The frequency of these alterations was about one Hz.

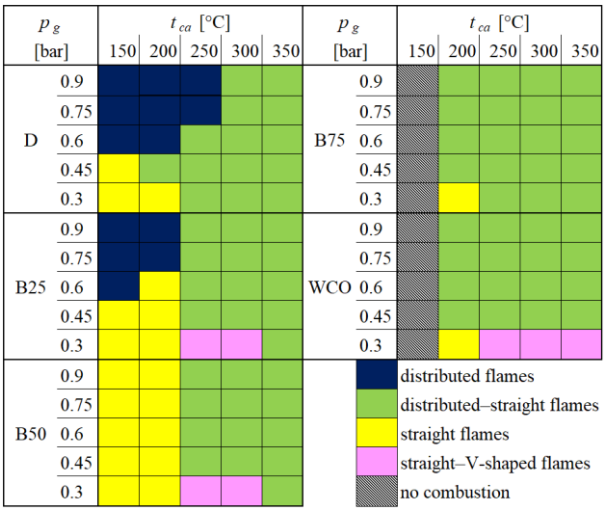

Fig. 4. Observed flame shapes.

Fig. 5. Typical flame images. D and B50 at t_{ca} = 200 °C, WCO at t_{ca} = 350 °C.

The yellow flame brush was typical for straight flames, notably affected by p_g. In Fig. 5, the first images of D and B50 show a typical luminous straight flame, which corresponds to a lower p_g, as the larger droplet sizes required more time to evaporate and mix with air. The flame becomes smaller at elevated p_g as the mixture quality improves.

As the two parameters, p_g and t_{ca}, were increased, the flame started to alter between straight and distributed shapes until the distributed combustion was stabilized. When increasing p_g in distributed combustion, the bluish flames are getting less luminous as it can be observed in Fig. 5 for D combustion. The bottom right image of WCO combustion shows a distributed flame, featuring purple color on its top, which is evidence of different reaction pathways due to the different fuel composition. It was also observed in CME combustion [17], and by Chong et al. [19] for sunflower biodiesel combustion.

The flame luminosity, and therefore, the flame shape can be determined based on the chemiluminescent spectrum. Figure 6 shows the chemiluminescent spectra of D flames at t_{ca} = 200 °C, B50 flames at t_{ca} = 200 °C and WCO flames at t_{ca} = 350 °C. The D flame at p_g = 0.3 bar was a luminous yellow flame, which is present in the spectra by a black body emission curve due to the soot particles. The flame at p_g = 0.45 bar is less luminous, however, the three typical radicals of hydrocarbon flames, OH* at around 309 nm, CH* at around 431 nm, and C_2* at around 516 nm, are clearly visible in the spectra. Distributed flames showed a low signal-to-noise ratio, hence, they are currently omitted.

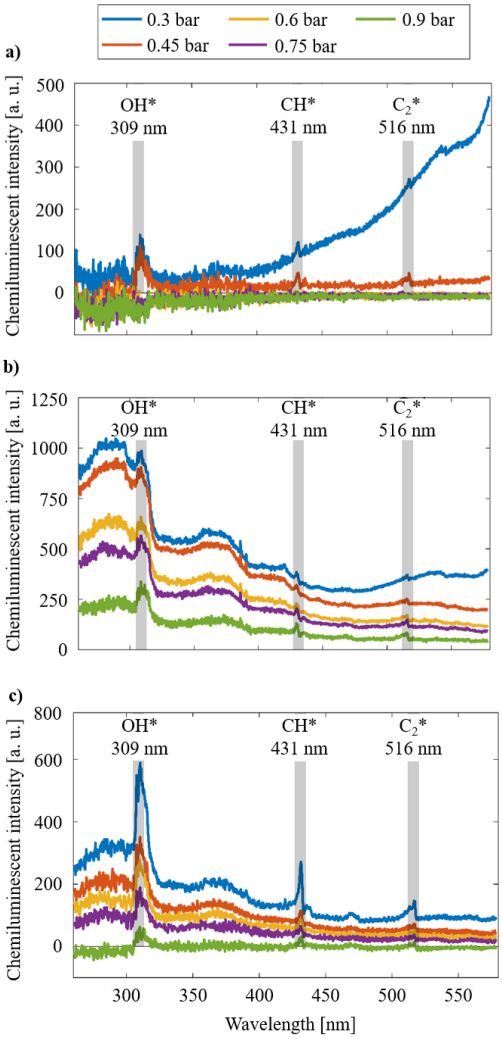

Fig. 6. Chemiluminescent spectra of **a)** D flames at t_{ca} = 200 °C, **b)** B50 flames at t_{ca} = 200 °C and **c)** WCO flames at t_{ca} = 350 °C.

The B50 flames were straight. The intensity of their spectra spectacularly decreases with an increase in p_g. Double spikes can be found in some of the spectra at around 390 nm wavelength, which indicates a CH* and a CH_2O* peak at around 387 and 395 nm, respectively.

In the case of WCO flame at p_g = 0.3 bar, an altering straight–V-shaped flame was observed. The chemiluminescent spectrum of this point has the highest intensity at all wavelengths; the strong intensity peaks of OH*, CH and C_2*, are clearly visible in the spectrum. As p_g is increased, the intensity of the spectra decreased, which led to a low signal-to-noise ratio to consistently detect CH and C_2 radicals.

The NO emission is shown in Fig. 7. Compared to the flame shape plots in Fig. 4, it can be concluded that the NO emission is highly sensitive to the shape. Distributed flames can be observed in the case of D and B25 combustion. This operating condition is found at the top left corner of D and B25 plots, where marginal NO emission was measured. As the flame becomes less stable and starts to alter between distributed and straight states, the NO emission suddenly increases. The effect of flame shapes on the NO emission in the case of the other fuels is visible as well. There is no sudden change in the NO emission since no distributed flame could stabilize, however, the ratio of distributed flames compared to straight flames in the altering region can be concluded based on the NO emission. Both p_g and t_{ca} influence the NO emission since lower flame temperature leads to decreased NO formation.

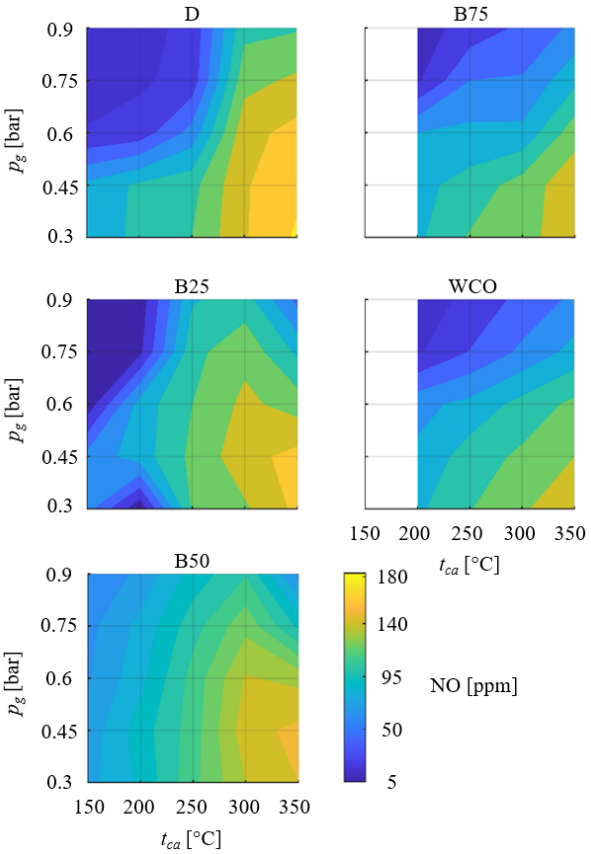

Fig. 7. NO emission.

An outlier can be found in the case of B25 at p_g = 0.3 bar and t_{ca} = 200 °C where a straight flame was observed. The lowest NO emission was measured for this blend, 5 ppm at p_g = 0.9 bar and t_{ca} = 150 °C at distributed combustion. For comparison, in the tested parameter range, the highest NO emission, 183 ppm, was measured

for D at p_g = 0.3 bar and t_{ca} = 350 °C when a straight luminous yellow flame was observed.

The CO emission is shown in Fig. 8. The CO emission remained below 10 ppm at almost all the parameter setups. However, some outliers can be found in the case of B75 and WCO combustion. It can be concluded that the combustion parameters did not notably affect the CO emission, and the combustion was complete in almost all cases. The mentioned points are most probably related to the high atomization pressure and incomplete combustion at some parts. Nevertheless, all these values are below the respective CO emission limitations set by the regulations in force.

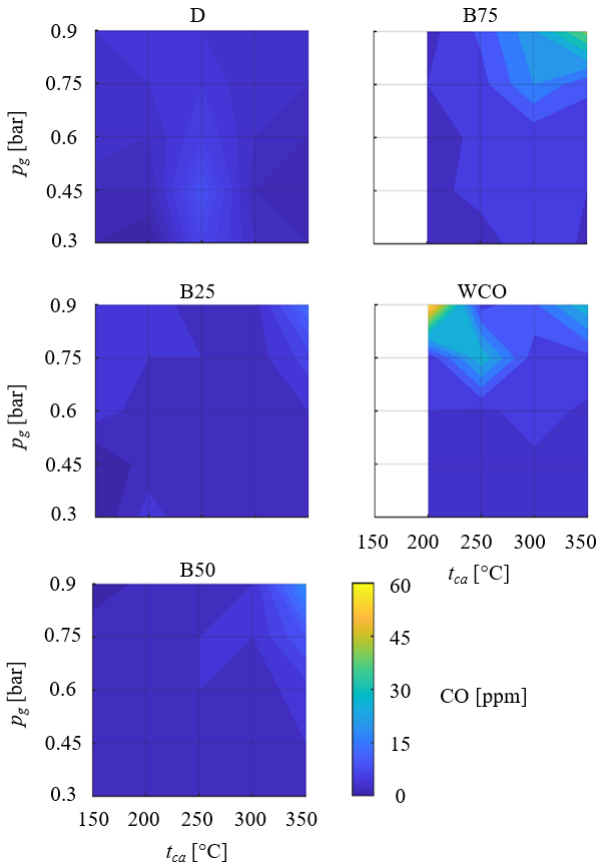

Fig. 8. CO emission.

Conclusions

Waste cooking oil (WCO), diesel fuel (D), and their blends of 25-50-75 V/V% WCO ratio (B25-B50-B75) were investigated in a novel, Mixture Temperature-Controlled (MTC) burner. The varied parameters were the atomizing gauge pressure (p_g) and the combustion air preheating temperature (t_{ca}) from 150 to 350 °C in 50 °C steps. The goal was to investigate if biodiesels with relatively low volatility can maintain distributed combustion at an equivalence ratio of 0.8.

Since p_g influences not only the mixture temperature but also the size of the fuel droplets, firstly, the fuel properties and the atomizing characteristics were evaluated. B75 and WCO combustion were possible only from t_{ca} = 200 °C.

During the combustion tests, three flame shapes were observed: V-shaped, straight, and distributed flames. At low p_g and t_{ca}, stable straight flames were present, characterized luminous yellow flame and moderate NO emission. At higher t_{ca}, altering flames between V and straight or straight and distributed shapes were observed. The highest overall air temperature resulted in the highest measured NO emission, which was 183 ppm for D combustion. If the distributed flame was stable, the NO emission was suddenly decreased, bottoming at 5 ppm for B25 combustion. CO emission remained below 10 ppm at almost all conditions.

The chemiluminescent spectra of straight flames were analyzed. The analysis of OH, CH, and C_2 radicals led to the conclusion that decreased flame intensity results in low signal-to-noise ratio to detect principally CH and C_2 radicals, while OH radicals were still observable.

The ultimate goal of the research was to exploit the combustion of WCO biodiesel-diesel blends focusing on distributed combustion. The application of an MTC burner in steady combustion chambers could radically decrease the NO emission.

Acknowledgments

The research reported in this paper was supported by the National Research, Development and Innovation Fund of Hungary, project №. OTKA-FK 124704 and New National Excellence Program of the Ministry for Innovation and Technology, project №.s ÚNKP-20-3-I-BME-182, and ÚNKP-20-3-II-BME-178.

References

[1] Chiaramonti D, Maniatis K. Security of supply, strategic storage and Covid19: Which lessons learnt for renewable and recycled carbon fuels, and their future role in decarbonizing transport? Appl Energy 2020;271:115216. https://doi.org/10.1016/j.apenergy.2020.115216.

[2] IEA. Transport: Improving the sustainability of passenger and freight transport 2020.

[3] Michalski J, Poltrum M, Bünger U. The role of renewable fuel supply in the transport sector in a future decarbonized energy system. Int J Hydrogen Energy 2019;44:12554–65. https://doi.org/10.1016/j.ijhydene.2018.10.110.

[4] Chen H-G, Zhang Y-HP. New biorefineries and sustainable agriculture: Increased food, biofuels, and ecosystem security. Renew Sustain Energy Rev 2015;47:117–32. https://doi.org/10.1016/j.rser.2015.02.048.

[5] Rezania S, Oryani B, Park J, Hashemi B, Yadav KK, Kwon EE, et al. Review on transesterification of non-edible sources for biodiesel production with a focus on economic aspects, fuel properties and by-product applications. Energy Convers Manag 2019;201:112155. https://doi.org/10.1016/j.enconman.2019.112155.

[6] Goh BHH, Chong CT, Ge Y, Ong HC, Ng JH,

Tian B, et al. Progress in utilisation of waste cooking oil for sustainable biodiesel and biojet fuel production. Energy Convers Manag 2020;223. https://doi.org/10.1016/j.enconman.2020.113296.
[7] De Feo G, Di Domenico A, Ferrara C, Abate S, Sesti Osseo L. Evolution of Waste Cooking Oil Collection in an Area with Long-Standing Waste Management Problems. Sustainability 2020;12:8578. https://doi.org/10.3390/su12208578.
[8] Kaushik LK, Muthukumar P. Thermal and economic performance assessments of waste cooking oil /kerosene blend operated pressure cook-stove with porous radiant burner. Energy 2020;206:118102. https://doi.org/10.1016/j.energy.2020.118102.
[9] Zhao N, Li B, Chen D, Ahmad R, Zhu Y, Li G, et al. Direct combustion of waste oil in domestic stove by an internal heat re-circulation atomization technology: Emission and performance analysis. Waste Manag 2020;104:20–32. https://doi.org/10.1016/j.wasman.2020.01.007.
[10] Ming C, Rizwanul Fattah IM, Chan QN, Pham PX, Medwell PR, Kook S, et al. Combustion characterization of waste cooking oil and canola oil based biodiesels under simulated engine conditions. Fuel 2018;224:167–77. https://doi.org/10.1016/j.fuel.2018.03.053.
[11] Attia AMA, Belal BY, El-Batsh HM, Moneib HA. Effect of waste cooking oil methyl ester – Jet A-1 fuel blends on emissions and combustion characteristics of a swirl-stabilized lean pre-vaporized premixed flame. Fuel 2020;267:117203. https://doi.org/10.1016/j.fuel.2020.117203.
[12] Lefebvre AH, Ballal DR. Gas turbine combustion. third. Boca Raton: CRC Press; 2010. https://doi.org/10.1002/1521-3773(20010316)40:6<9823::AID-ANIE9823>3.3.CO;2-C.
[13] Correa SM. A Review of NOx Formation Under Gas-Turbine Combustion Conditions. Combust Sci Technol 1993;87:329–62. https://doi.org/10.1080/00102209208947221.
[14] Cavaliere A, De Joannon M. Mild combustion. Prog Energy Combust Sci 2004;30:329–66. https://doi.org/10.1016/j.pecs.2004.02.003.
[15] Xing F, Kumar A, Huang Y, Chan S, Ruan C, Gu S, et al. Flameless combustion with liquid fuel : A review focusing on fundamentals and gas turbine application. Appl Energy 2017;193:28–51. https://doi.org/10.1016/j.apenergy.2017.02.010.
[16] Józsa V. Mixture temperature-controlled combustion: A revolutionary concept for ultra-low NOx emission. Fuel 2021;291:120200. https://doi.org/10.1016/j.fuel.2021.120200.
[17] Józsa V, Hidegh G, Kun-Balog A, Ng J-H, Chong CT. Ultra-low emission combustion of diesel-coconut biodiesel fuels by a mixture temperature-controlled combustion mode. Energy Convers Manag 2020;214:112908. https://doi.org/10.1016/j.enconman.2020.112908.
[18] Urbán A, Malý M, Józsa V, Jedelský J. Effect of liquid preheating on high-velocity airblast atomization: From water to crude rapeseed oil. Exp Therm Fluid Sci 2019;102:137–51. https://doi.org/10.1016/j.expthermflusci.2018.11.006.
[19] Chong CT, Chiong M, Ng J, Lim M, Tran M-V, Valera-Medina A, et al. Oxygenated sunflower biodiesel: Spectroscopic and emissions quantification under reacting swirl spray conditions. Energy 2019;178:804–13. https://doi.org/10.1016/j.energy.2019.04.201.